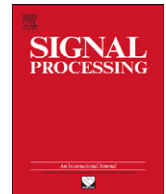




ELSEVIER

Contents lists available at ScienceDirect

## Signal Processing

journal homepage: [www.elsevier.com/locate/sigpro](http://www.elsevier.com/locate/sigpro)

Fast communication

## Discrete-time chaotic systems synchronization performance under additive noise

M. Eisenkraft<sup>a,\*</sup>, A.M. Batista<sup>b,\*</sup><sup>a</sup> Centro de Engenharia, Modelagem e Ciências Sociais Aplicadas, Universidade Federal do ABC, 09210-170 Santo André, SP, Brazil<sup>b</sup> Departamento de Matemática e Estatística, Universidade Estadual de Ponta Grossa, 84030-900 Ponta Grossa, PR, Brazil

## ARTICLE INFO

## Article history:

Received 6 October 2010

Accepted 23 January 2011

Available online 4 February 2011

## Keywords:

Maps

Noise

Synchronization

## ABSTRACT

In recent decades many articles have discussed the possibilities of chaos applied in communications. However, the vast majority consider in practical terms the ideal channel condition, which is clearly a restricting condition. Some papers show that when there is an additive noise, the synchronization error often disrupts communication. In this work, we present results of a comparison between synchronization error due to additive Gaussian noise when the transmitter and receiver are implemented by single or coupled maps.

© 2011 Published by Elsevier B.V.

## 1. Introduction

Chaotic signals are characterized by a deterministic and aperiodic behavior, as well as sensitive dependence on initial conditions [1]. Their applications have been considered in a variety of areas [2]. Signal Processing and Telecommunications are not exception specially after the seminal work [3]. Applications of chaos ranging from digital and analog modulation to cryptography, to pseudorandom sequences generation and watermarking, among many others, have been proposed [4–7]. Chaos may be observed in devices used in signal processing as nonlinear adaptive filters and phase-locked loop networks [8–11].

Due to their properties chaotic signals turn out to occupy a wide bandwidth and to have impulsive autocorrelation. Furthermore, the cross-correlations between signals generated by different initial conditions present low values [4,5,7,12]. These characteristics have been behind the rationale for using chaotic signals as candidates in spreading signal information.

The application of the chaotic signals to modulate independent narrowband sources leads to systems that transmit signals with increased bandwidths and lower levels of power spectral density in fashion similar to that of a spread spectrum system [13]. This fact endows them with similar qualities namely (i) they are difficult to intercept for an unauthorized person; (ii) they are easily hidden, i.e. for an unauthorized person, it is difficult to even detect their presence in many cases; (iii) they are resistant to jamming; and (iv) they provide a measure of immunity to distortion due to multipath propagation.

The most part of the proposed chaos-based communication systems is based on chaos synchronization of a master–slave structure where the slave system is driven by a signal derived from the master [3,14].

The proposed systems work very well in ideal environments, although the presence of noises and distortions in the channel bring unsatisfactory results when chaotic synchronization is used, due to fact of the sensitive dependence on initial conditions that characterize chaotic signals [4,15,16].

In this paper we numerically investigate an alternative model to decrease the master–slave synchronization error when there is additive white Gaussian noise between master and slave: using coupled lattices instead of coupled single maps.

\* Corresponding authors.

E-mail addresses: [marcio.eisenkraft@ufabc.edu.br](mailto:marcio.eisenkraft@ufabc.edu.br) (M. Eisenkraft), [batista@interponta.com.br](mailto:batista@interponta.com.br) (A.M. Batista).

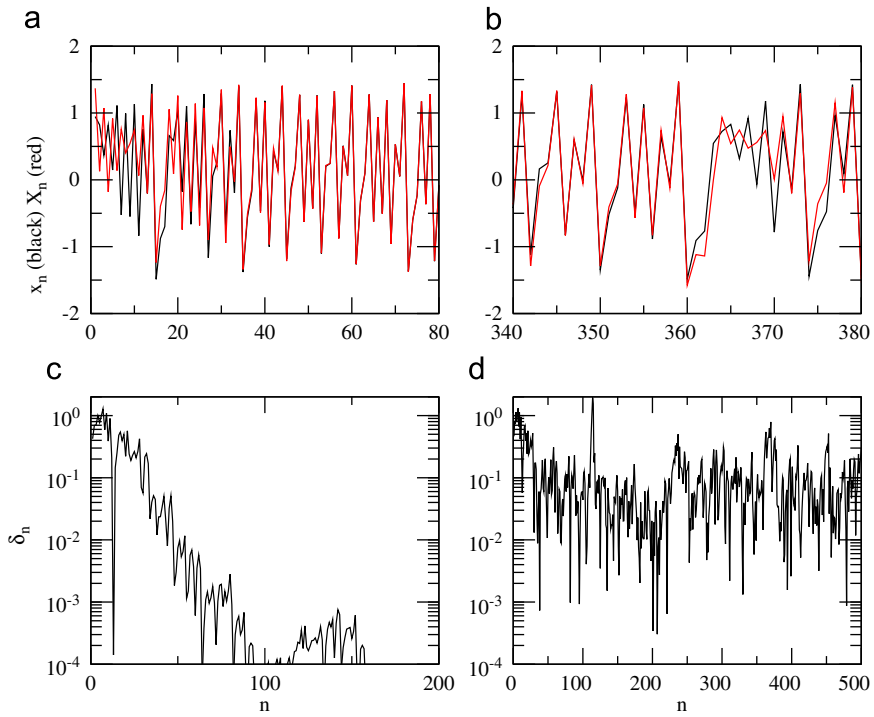


**Fig. 1.** Master–slave system considering  $\varepsilon_t = 0.3$ , (a) and (c) without noise, (b) and (d) SNR=8. (For interpretation of the references to color in this figure legend, the reader is referred to the web version of this article.)

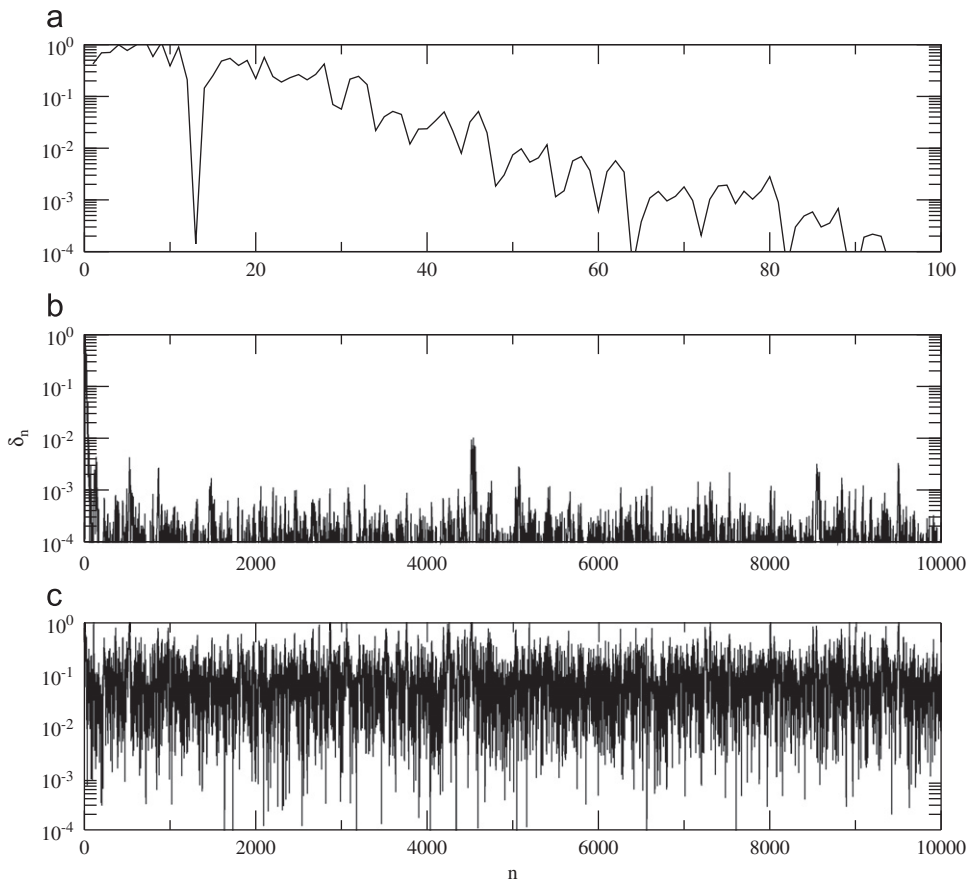


**Fig. 2.** Master–slave system considering  $\varepsilon_t = 0.3$ , (a) without noise, (b) SNR=8000 and (c) SNR=8.

This paper is organized as follows: in Section 2 we present the considered models and in Section 3 we analyze synchronization error as a function of the signal-to-noise ratio, of the coupling strength and of the number of maps in the lattices. Finally our conclusions are left to Section 4.

**2. Single maps and lattices master–slave synchronization**

As a first model, we consider two coupled 3D-Henon maps [17,18] in a master–slave configuration with additive noise in the link between them. This way, the coupling is given by

$$x_{n+1} = -ax_n^2 + z_n + 1, \tag{1}$$

$$y_{n+1} = -bx_n, \tag{2}$$

$$z_{n+1} = bx_n + y_n, \tag{3}$$

$$X_{n+1} = (1-\varepsilon)(-aX_n^2 + Z_n + 1) + \varepsilon_l I_n, \tag{4}$$

$$Y_{n+1} = -bX_n, \tag{5}$$

$$Z_{n+1} = bX_n + Y_n, \tag{6}$$

$$I_n = f(x_n, z_n) + r_n, \tag{7}$$

where we have used lower-case letters for the master states and capital letters for the slave states,  $f(x,z) = -ax^2 + z + 1$ ,  $0 \leq \varepsilon_l \leq 1$  is the coupling strength,  $r_n$  is zero-mean Additive White Gaussian Noise (AWGN) with variance  $\sigma^2$  and  $n=0,1,2,\dots$  is the discrete time.

Considering  $a=1.07$  and  $b=0.3$  the three-dimensional generalization of the Henon map presents chaotic orbits for almost all initial conditions in the unity sphere [17,18].

The synchronization error dynamics between the two systems is given by

$$\delta_n = |x_n - X_n|, \tag{8}$$

and we considered that synchronization occurs when  $\delta_n < 10^{-3}$ . For the chosen parameters, it can be shown that  $\delta_n \rightarrow 0$  as  $n \rightarrow \infty$  if  $\sigma = 0$  [19].

For measuring the noise intensity in the channel we use the popular Signal-to-Noise Ratio (SNR) defined as the mean power of the transmitted signal  $I_n$  divided by  $\sigma^2$ . This way, the higher the SNR, the lower the relevance of the noise in the channel. In an ideal situation,  $\text{SNR} = \infty$ .

Fig. 1(a) displays the temporal evolution of the state variable of the master (black line) and slave (red line) map with  $\varepsilon_l = 0.3$  and no noise ( $\sigma^2 = 0$ ). Fig. 1(c) shows the synchronization error and in this case we can see that the two 3D-Henon synchronize after a transient time.

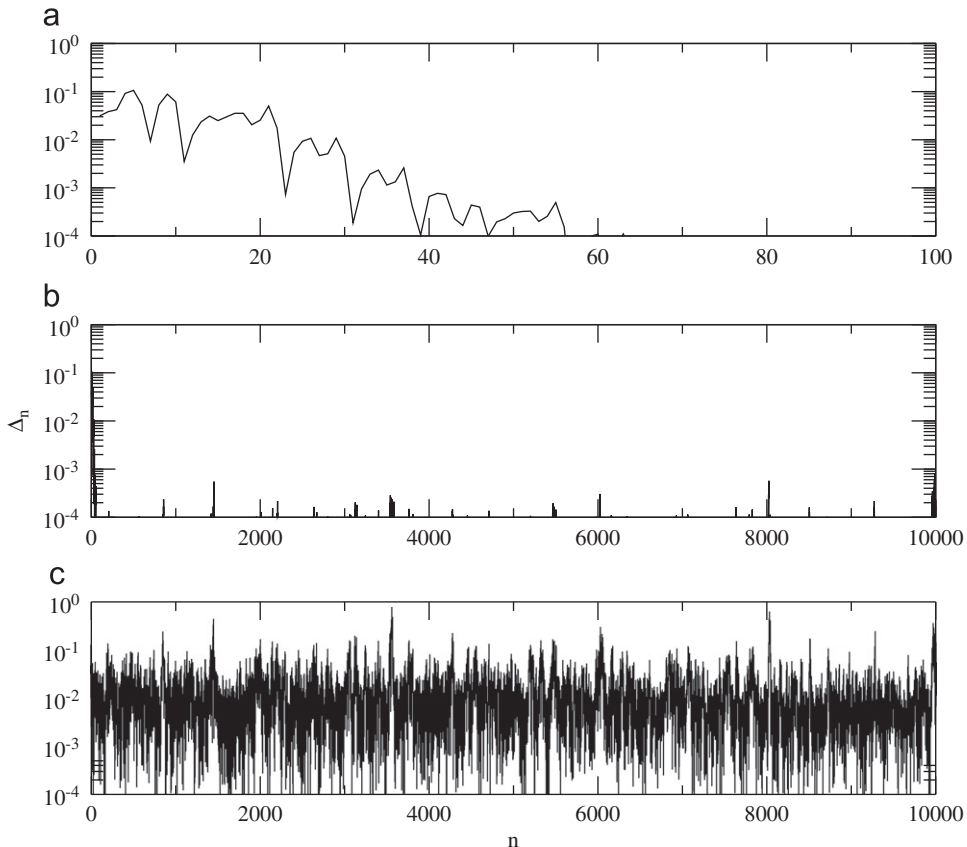


**Fig. 3.** Master–slave system considering unidirectional coupling between two global coupled map lattices for  $N=10$ ,  $\varepsilon_1 = \varepsilon_2 = 0.7$ ,  $\varepsilon_l = 0.3$ , (a) without noise, (b)  $\text{SNR}=8000$  and (c)  $\text{SNR}=8$ .

Similarly, Figs. 1(b) and (d) show the synchronization performance at SNR=8, where the synchronization is destroyed by the channel noise.

Fig. 2 shows the behavior of the synchronization error for different values of the SNR. Decreasing SNR the maps pass from synchronized to nonsynchronized behavior exhibiting values of the synchronization error with irregular oscillations.

As an option to increase the robustness of synchronization with respect to channel noise, let us consider now coupled maps lattices instead of single maps in the master–slave configuration. Coupled maps lattices are the prototype of spatially extended dynamical systems, that presents discrete space and time, while the state variable is continuous. We consider two lattices where each one presents a global coupling prescription, and the coupling between the lattices is unidirectional. The coupling is given by

$$x_{n+1}^{(i)} = (1-\varepsilon_1)(-ax_n^{(i)2} + z_n^{(i)} + 1) + \frac{\varepsilon_1}{N} \sum_{i=1}^N f(x_n^{(i)}, z_n^{(i)}), \quad (9)$$

$$y_{n+1}^{(i)} = -bx_n^{(i)}, \quad (10)$$

$$z_{n+1}^{(i)} = bx_n^{(i)} + y_n^{(i)}, \quad (11)$$

$$X_{n+1}^{(i)} = (1-\varepsilon_2)(-aX_n^{(i)2} + Z_n^{(i)} + 1) + \frac{\varepsilon_2}{N} \sum_{i=1}^N f(X_n^{(i)}, Z_n^{(i)}) + \frac{\varepsilon_1}{N} I_n, \quad (12)$$

$$Y_{n+1}^{(i)} = -bX_n^{(i)}, \quad (13)$$

$$Z_{n+1}^{(i)} = bX_n^{(i)} + Y_n^{(i)}. \quad (14)$$

$$I_n = \sum_{i=1}^N f(x_n^{(i)}, z_n^{(i)}) - \sum_{i=1}^N f(X_n^{(i)}, Z_n^{(i)}) + r_n. \quad (15)$$

where again we have used lower-case letters for the master states and capital letters for the slave states. The superscript index  $i=1, \dots, N$  identifies a particular map in the  $N$ -maps lattice. We define the synchronization error for the two coupled lattices as

$$\Delta_n = \frac{1}{N} \left| \sum_{i=1}^N x_n^{(i)} - \sum_{i=1}^N X_n^{(i)} \right| \quad (16)$$

and we say that master and slave synchronize if  $\Delta_n < 10^{-3}$ .

Fig. 3 shows time behaviors of  $\Delta_n$  for different SNR values. Again the synchronization error increases when the SNR decreases but the oscillations of the error present amplitudes no greater than the values obtained in the single map case for the same parameters, shown in Fig. 2. Consequently, coupled lattices are more robust to noise than two unidirectionally coupled maps.

In the next section we numerically analyze the synchronization error as function of the coupling strength and of the number of maps in the lattice.

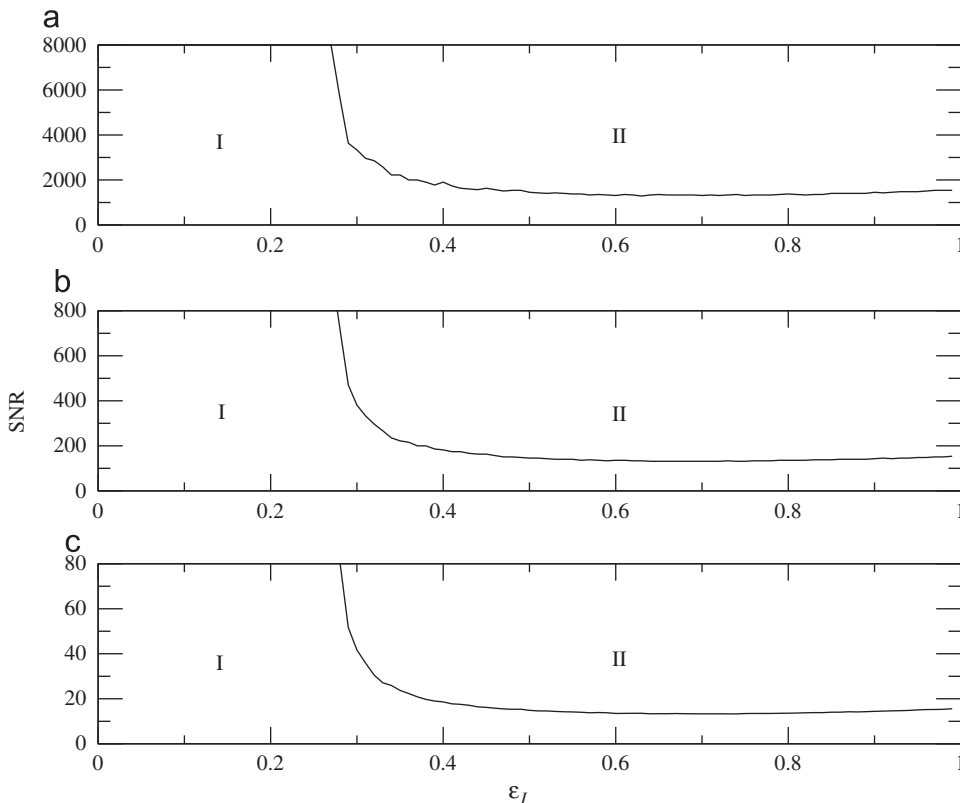
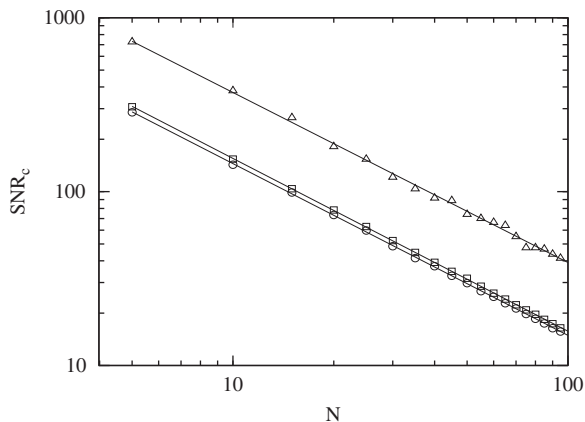


Fig. 4. Region I represents the values of SNR and the coupling strength in that the system does not present synchronization, while in the region II there is synchronization. (a) two 3D-Henon, (b) two lattices with 10 3D-Henon each one and (c) two lattices with 100 3D-Henon each one.



**Fig. 5.** Vertical length of the nonsynchronization region versus lattice size, for  $\varepsilon_l = 0.3$  (triangles),  $\varepsilon_l = 0.5$  (circles) and  $\varepsilon_l = 1.0$  (squares). We can observe a power-law of  $\text{SNR}_c$  as  $N$  grows with a slope  $\approx -1$ .

### 3. Lattices synchronization performance

Fig. 4 illustrates how master–slave synchronization of two lattices depends on the coupling strength  $\varepsilon_l$ , the SNR and the number of maps in the lattices,  $N$ . The Region I corresponds to the nonsynchronized states considered when in a time interval ( $5000 \leq n \leq 50\,000$ ) we have 5% or more of the values presenting (a)  $\delta_n > 10^{-3}$  for single 3D-Henon coupled maps, (b)  $\Delta_n > 10^{-3}$  for two lattices with 10 3D-Henon each one and (c)  $\Delta_n > 10^{-3}$  for two lattices with 100 3D-Henon each one. Otherwise, in the Region II occurs the synchronized state.

The synchronization region depends on the lattice size. To study this dependence we define the critical SNR,  $\text{SNR}_c$ , as the maximum value of the SNR that allows synchronization in the sense described in the previous paragraph.

Fig. 5 shows the  $\text{SNR}_c$  as a function of the lattice size  $N$  for  $\varepsilon_l = 0.3$  (triangles),  $\varepsilon_l = 0.5$  (circles) and  $\varepsilon_l = 1.0$  (squares), where we observe that the value of  $\text{SNR}_c$  decreases following a power-law with slope  $\approx -1$ . We can also infer from this figure that for  $\varepsilon_l \geq 0.5$  the coupling strength almost does not influence  $\text{SNR}_c$ .

### 4. Conclusions

In this paper we numerically compared single map and lattices in terms of master–slave synchronization error under AWGN. The synchronization is analyzed as function of the coupling strength and the SNR.

We have observed that the synchronization is more robust to noise when the number of maps in the lattice increases. The critical coupling strength does not depend on the lattice size. Moreover, the dependence of the critical SNR

with the lattice size can be fitted by a power-law, where the slope is approximately equal to  $-1$ .

These results may imply that using lattices instead of single maps can be a way to improve performance of chaos-based communication systems in more realistic environments.

As future works we will extend this results to continuous-time signals and systems, as well as we will look for analytical results.

### Acknowledgements

This study was possible by partial financial support from the following Brazilian government agencies: CNPq, CAPES and Fundação Araucária.

### References

- [1] K.T. Alligood, T.D. Sauer, J.A. Yorke, Textbooks in mathematical sciences, in: *Chaos: An Introduction to Dynamical Systems*, Springer-Verlag, New York, 1997.
- [2] S.H. Strogatz, *Nonlinear Dynamics and Chaos: With Applications to Physics, Biology, Chemistry and Engineering*, Perseus Books Group, 2001.
- [3] L. Pecora, T. Carroll, Synchronization in chaotic systems, *Physical Review Letters* 64 (8) (1990) 821–824.
- [4] M.P. Kennedy, G. Setti, R. Rovatti (Eds.), *Chaotic Electronics in Telecommunications*, CRC Press Inc., Boca Raton, FL, USA, 2000.
- [5] M. Kennedy, G. Kolumban, Digital communications using chaos, *Signal Processing* 80 (7) (2000) 1307–1320.
- [6] S. Tsekeridou, V. Solachidis, N. Nikolaidis, A. Nikolaidis, A. Tefas, I. Pitas, Statistical analysis of a watermarking system based on Bernoulli chaotic sequences, *Signal Processing* 81 (6) (2001) 1273–1293.
- [7] P. Stavroulakis (Ed.), *Chaos Applications in Telecommunications*, CRC Press Inc., Boca Raton, FL, USA, 2005.
- [8] T. Endo, L. Chua, Chaos from phase-locked loops, *IEEE Transactions on Circuits and Systems* 35 (8) (1998) 987–1003.
- [9] B.A. Harb, A.M. Harb, Chaos and bifurcation in a third-order phase locked loop, *Chaos, Solitons & Fractals* 19 (3) (2004) 667–672.
- [10] M.S. Tavazoei, M. Haeri, Chaos in the apfm nonlinear adaptive filter, *Signal Processing* 89 (5) (2009) 697–702.
- [11] L.H.A. Monteiro, A.C. Lisboa, M. Eisenkraft, Route to chaos in a third-order phase-locked loop network, *Signal Processing* 89 (8) (2009) 1678–1682.
- [12] I. Djurovic, V. Rubezic, Chaos detection in chaotic systems with large number of components in spectral domain, *Signal Processing* 88 (9) (2008) 2357–2362.
- [13] B.P. Lathi, *Modern Digital and Analog Communication Systems*, third ed., Oxford University Press, Inc., New York, NY, USA, 1998.
- [14] T. Carroll, L. Pecora, Synchronizing chaotic circuits, *IEEE Transactions on Circuits and Systems* 38 (4) (1991) 453–456.
- [15] F.C.M. Lau, C.K. Tse, *Chaos-Based Digital Communication Systems*, Springer, Berlin, 2003.
- [16] C. Williams, Chaotic communications over radio channels, *IEEE Transactions on Circuits and Systems I: Fundamental Theory and Applications* 48 (12) (2001) 1394–1404.
- [17] D.L. Hitzl, F. Zele, An exploration of the hnon quadratic map, *Physica D: Nonlinear Phenomena* 14 (3) (1985) 305–326.
- [18] K. Stefanski, Modelling chaos and hyperchaos with 3-d maps, *Chaos, Solitons & Fractals* 9 (1–2) (1998) 83–93.
- [19] M. Eisenkraft, R.D. Fanganiello, L. Baccalá, Synchronization of a discrete-time chaotic systems in bandlimited channels, *Mathematical Problems in Engineering* 2009 (2009) 1–15.